

LA-UR- 08-1202

Approved for public release;  
distribution is unlimited.

*Title:*

Crystal Grain Growth During Room Temperature High Pressure Martensitic  $\alpha$  to  $\omega$  Transformation in Zirconium

*alpha omega*

*Author(s):*

Nenad Velisavljevic, Lewis L. Stevens, Gary N. Chesnut, Dana M. Dattelbaum

*Intended for:*

Review by authors, then journal publication



Los Alamos National Laboratory, an affirmative action/equal opportunity employer, is operated by the Los Alamos National Security, LLC for the National Nuclear Security Administration of the U.S. Department of Energy under contract DE-AC52-06NA25396. By acceptance of this article, the publisher recognizes that the U.S. Government retains a nonexclusive, royalty-free license to publish or reproduce the published form of this contribution, or to allow others to do so, for U.S. Government purposes. Los Alamos National Laboratory requests that the publisher identify this article as work performed under the auspices of the U.S. Department of Energy. Los Alamos National Laboratory strongly supports academic freedom and a researcher's right to publish; as an institution, however, the Laboratory does not endorse the viewpoint of a publication or guarantee its technical correctness.

# Crystal Grain Growth During Room Temperature High Pressure Martensitic $\alpha$ to $\omega$ Transformation in Zirconium

Nenad Velisavljevic, Lewis L. Stevens, Gary N. Chesnut, and Dana M. Dattelbaum

Los Alamos National Laboratory, Los Alamos, New Mexico 87544

Systematic increase in transition pressure with increase in interstitial impurities is observed for the martensitic  $\alpha \rightarrow \omega$  structural phase transition in Zr. Significant room temperature crystal grain growth is also observed for the two highest purity samples at this transition, while in the case of the lowest purity sample interstitial impurities obstruct grain growth even as the sample is heated to 1279 K. Our results show the importance of impurities in controlling structural phase stability and other mechanical properties associated with the  $\alpha \rightarrow \omega$  structural phase transition.

PACS numbers: 61.50Ks, 8130Kf, 9160Gf

Mechanical properties of materials are greatly influenced by structural phase transitions, which can occur during both high temperature and high pressure applications. One of the most studied structural phase transitions are the diffusionless martensitic phase transitions. Martensitic transitions occur in a broad range of materials, such as iron [1, 2], group IV metals: titanium (Ti), zirconium (Zr), and hafnium (Hf) [3], and shape memory alloys [4]. In group IV metals room temperature compression leads to a martensitic transformation from a ductile  $\alpha$  to a brittle  $\omega$  phase at  $\sim 8$  GPa for Ti,  $\sim 8$  GPa for Zr, and 14 GPa for Hf. The  $\alpha \rightarrow \omega$  phase boundary decreases to lower pressures at

high temperatures [5] and can severely limit the use of group IV metals in industrial applications. Impurities also play an important role on the phase boundary as they can either aid or suppress the  $\alpha \rightarrow \omega$  transition. Substitutional impurities such as aluminum can decrease d-electron concentration and increase the stability of  $\alpha$  phase to higher pressures, on the other hand d-electron rich impurities like molybdenum increase d-electron concentration and decrease the  $\alpha \rightarrow \omega$  transition pressure [6]. In the case of interstitial impurities results of ab initio calculations show that oxygen, nitrogen and carbon occupying the hexahedral and octahedral sites increase the energy barrier and block the  $\alpha \rightarrow \omega$  transformation [7].

In addition to their influence on the  $\alpha \rightarrow \omega$  transition pressure impurities also raise other questions as to their effect on kinetics and nucleation and growth of  $\omega$  phase, as well as other high pressure phases of group IV metals. Using electrical resistivity technique, isothermal compression studies indicate that the growth of  $\omega$  phase in Ti is very sluggish [8]. Furthermore, in examining the possibility of high-pressure formation of bulk metallic glass in elemental Zr and Ti it was shown that compressing ultrahigh purity Zr to 8.3 GPa and subsequently heating to 650°C can lead to large grain growth [9]. The fairly smooth x-ray diffraction rings of Zr become very spotty during the  $\omega \rightarrow \beta$ (bcc) as reported in ref. 9. Change in crystallite size is very important as it can greatly influence measured quantities such as elastic moduli and it can also affect materials ability to plastically deform [10]. Kinetics and grain growth effects are experimentally challenging to detect at high pressures. Historically a majority of high pressure experimental studies have been performed using energy dispersive x-ray diffraction (EDXD) technique. With EDXD a

solid-state point detector measures diffraction only over a limited area of a two

dimensional diffraction pattern and grain growth effects could easily be missed [9]. It is therefore advantageous to use angle dispersive x-ray diffraction (ADX) technique which allows for the whole two dimensional diffraction pattern to be observed.

Likewise, kinetics studies are also difficult due to the time delay of increasing pressure and the time it takes to record ADXD or EDXD spectra, which can depend on the diffraction technique used, x-ray source, and the type of detector used. For this reason static high pressure phase transition kinetics studies have predominantly been investigated using the electrical resistance measurements technique, as was done in Ti study [8]. However advancements in synchrotron radiation sources as well as increased availability of ADXD equipped beamlines is allowing for further insight into the behavior of materials at high pressures. In this letter we report on measurements which show a direct correlation between increase in  $\alpha \rightarrow \omega$  phase transition pressure and increase in interstitial impurity concentration. Furthermore, we also show that initial sample texture can lead to significant grain growth at the onset of room temperature and high pressure  $\alpha \rightarrow \omega$  phase transition.

Multiple experiments were performed on Zr having 25  $\mu\text{m}$  initial grain size and of various purity, as shown in Table I. All three samples were subjected to static high pressures in a diamond anvil cell under both hydrostatic, using methanol-ethanol (4:1) mixture, and non-hydrostatic conditions. Since the stress distribution inside the sample chamber, and ultimately the pressure over which the plastic deformation of the sample occurs, can depend on the anvil culet size [10] we have performed all studies using an

anvil with a 300  $\mu\text{m}$  diameter culet and samples loaded in a 90  $\mu\text{m}$  hole drilled in a pre-indent spring steel gasket. In all cases ADXD technique was used and pressure was determined based on the room temperature equation of state of copper [11, 12]. All three samples were investigated at room temperature and up to 15 GPa, and in addition the lowest purity sample was also investigated up to 11 GPa and 1279 K. Experiments were performed at beamline 16 ID-B and 16 BM-D, of HPCAT, Advanced Photon Source (APS), at Argonne National Laboratory and at beamline B2 at Cornell's High Energy Synchrotron Source (CHESS).

Initially all three samples are observed to be in  $\alpha$  phase, hcp, at RTP and having lattice parameter  $a_0 = 3.232 \pm 0.002 \text{ \AA}$  and  $c_0 = 5.146 \pm 0.002 \text{ \AA}$  ( $c/a = 1.593$ ) and volume/atom =  $23.270 \text{ \AA}^3$ . As the pressure is increased all three samples, under both hydrostatic and non-hydrostatic conditions, undergo a structural phase transition from  $\alpha$  to  $\omega$  (hexagonal with three atoms per unit cell) phase [3]. We also observe that for all three samples this structural phase transition is accompanied by  $\sim 1.5\%$  discontinuous volume decrease and occurs systematically at a lower pressure when samples were subjected to non-hydrostatic versus hydrostatic conditions, Table I. This is consistent with previous studies, which showed that under non-hydrostatic conditions shear stresses drive the  $\alpha \rightarrow \omega$  structural phase transition and reduce the transition pressure in Ti [13]. In the case of ZrI and ZrII we also observe that the diffraction images become very grainy during room temperature  $\alpha \rightarrow \omega$  transition. Figure 1 shows the ADXD pattern collected from ZrII sample at onset of  $\alpha \rightarrow \omega$  transition at 7.5 GPa under hydrostatic conditions. As can be seen in figure 1, diffraction from  $\omega$  phase consists of numerous Bragg spots, rather

than smooth diffraction rings as observed for the  $\alpha$  phase and the copper pressure marker.

The occurrence of few diffraction spots indicates that the  $\omega$  phase consists of several single crystals, rather than many smaller crystals. Room temperature grain growth during the  $\alpha \rightarrow \omega$  transition is very unusual, as grain growth is typically attained in materials through high temperature treatment which leads to a decrease in defect density by reduction of surface area per unit volume. As mentioned, both ZrI and ZrII are observed to have large grain growth during the  $\alpha \rightarrow \omega$  transition, while full diffraction rings are ~~not~~ observed, suggesting no significant grain size increase, for the lowest purity zirconium, ZrIII. Figure 2 shows the image plate recording and the integrated diffraction pattern for the three samples during the start of the  $\alpha \rightarrow \omega$  transition under non-hydrostatic conditions. Due to the sluggish growth rate of  $\omega$  phase, as reported for Ti [8], multiple ADXD spectra were recorded at constant pressure at each pressure point on approach, during, and after the  $\alpha \rightarrow \omega$  transition. This allowed us to better determine the onset of this transition, as well as the transition kinetics. Furthermore, diffraction patterns were collected over a sufficiently long enough period as to allow for possible formation of any smooth diffraction rings to be observed. However, as can be seen in figure 3 (a)-(c), when consecutive diffraction patterns are recorded at constant pressure we do not see the formation of smooth diffraction rings for the  $\omega$  phase over a period of ~20 minutes (five minutes per spectra plus ~2 minutes in-between spectra). At the same time extremely slow growth of  $\omega$  phase in the  $\alpha$  matrix can be seen in the same figure, as the relative density of Bragg spots is observed to increase with time and stabilizes after ~20 minutes. Diffraction pattern from the  $\omega$  phase continues to be spotty, although becoming

somewhat smoother as the pressure is increased up to 13.4 GPa, figure 3 (c), and then once the pressure is released to ambient pressure, figure 3 (d).

The room temperature grain growth in our experiments occurs at a much lower temperature and during the  $\alpha \rightarrow \omega$  transition compared to the grain growth observed in Zr by T. Hattori et al. [9] at 8.3 GPa and 650°C at the onset of  $\omega \rightarrow \beta$  transition. The very unusual formation of several single crystals at a temperature that is less than half the melting temperature was attributed to anomalous lattice dynamics and the resulting anomalous fast self diffusion associated with bcc Zr and Ti [9]. Although purity of Zr sample investigated by T. Hattori et al. [9] using a multianvil high-pressure apparatus is reported to be same as our ZrI sample, no information is given about the initial sample texturing, which could be responsible for the room temperature grain growth observed in our experiments. All three Zr samples in this study were upset forged and clock rolled followed by annealing at 550°C, which resulted in a strongly textured plate with the normal nearly aligned with the c-axis [14]. Based on the lowest energy barrier pathway a transition model for the titanium  $\alpha \rightarrow \omega$  transformation has been proposed [15], in which a direct six-atom transformation proceeds without a metastable intermediate phase and can possibly lead to the resulting  $\omega$  matrix being oriented to the original  $\alpha$  matrix such that  $(0001)_{\alpha} \parallel (0\bar{1}11)_{\omega}$  and  $[11\bar{2}0]_{\alpha} \parallel [01\bar{1}1]_{\omega}$ . Since sample history is known to effect the  $\alpha \rightarrow \omega$  transformation pressure in Ti [8] a more detailed comparison of the starting sample texturing and the resulting influence on relation between  $\alpha$ - $\omega$  crystal orientation needs to be made in order to resolve the discrepancy between the observed grain growth in our experiments and what was reported by T. Hattori et al. [9]. In addition it should also be

noted that grain growth during room temperature  $\alpha \rightarrow \omega$  transition observed in our experiments for ZrI and ZrII occurs under both hydrostatic and non-hydrostatic sample conditions. By performing experiments under hydrostatic conditions texturing effects, which can also develop at high pressures, can be reduced and in addition sample conditions would more closely resemble conditions of a sample subjected to high pressures in a multianvil apparatus.

Impurities play a significant role in controlling grain growth in Zr. Both  $\alpha$  and  $\omega$  are higher symmetry structures, however the atomic packing factor decreases significantly from  $\sim 0.74$  for  $\alpha$  phase down to  $\sim 0.54$  for  $\omega$  phase. The smaller packing ratio ultimately results in fewer atoms at the grain boundary which can affect the grain boundary energy, and in turn produce conditions suitable for grain boundary migration and grain growth. However, increase in interstitial impurity concentration as in the case of ZrIII will lead to an increase in atomic density, especially at the grain boundary, and a decrease in the nearest neighbor distance [15], resulting in considerable limitation on grain boundary mobility. Remarkably, even though grain growth is observed at room temperature for ZrI and ZrII no significant grain growth is observed for ZrIII even at high temperatures.

Figure 4 shows the image plate recording for ZrIII collected at 1279 K at 11 GPa. Initially pressure was increased at room temperature up to 11 GPa, start of the  $\alpha \rightarrow \omega$  transition, and then held constant as the sample was heated up to 1279 K. Above 1150 K we observe the  $\omega \rightarrow \beta$  structural phase transition, however the diffraction rings appear to be fairly smooth and remain so up to the highest temperature attained.

In conclusion we show that Zr metal undergoes large grain growth during room temperature high pressure  $\alpha \rightarrow \omega$  transition. Grain growth appears to be dependant on the initial texturing of the sample, and can be hampered by interstitial impurities present in the sample, which also increase the energy barrier of the  $\alpha \rightarrow \omega$  transformation and shift the phase boundary to higher pressures. In ZrI and ZrII grain growth was consistently observed independent of the x-ray beam diameter, which ranged from  $\sim 10 \mu\text{m}$  up to  $\sim 50 \mu\text{m}$ , and under both hydrostatic and non-hydrostatic conditions, while no significant grain size increase was detected for ZrIII under the same experimental conditions. The observed grain growth in Zr metal also raises more general questions regarding room temperature high pressure structural phase transitions. Many studies have shown that preferred orientation and, as in case of hcp metals such as iron [16], basal plane texture can develop during compression in a diamond anvil cell. Furthermore, since hcp, along with fcc crystal structure, has the highest atomic packing factor any subsequent structural phase transition can result in the lowering of atomic packing factor which, as seen here, can provide suitable condition for crystal grain growth even at room temperature.

## ACKNOWLEDGMENTS

Portion of this work was performed at HPCAT (Sector 16), Advanced Photon Source (APS), Argonne National Laboratory. HPCAT is supported by DOE-BES, DOE-NSA, NSF, and the W.M. Keck Foundation. APS is supported by DOE-BES, under Contract No. DE-AC02-06CH11357. Part of the work was also performed at B2 beamline at Cornell High Energy Synchrotron Source (CHESS) which is supported by the NSF and the NIH/National Institute of General Medical Sciences under NSF award

DMR-0225180. LANL is operated by LANS, LLC for the DOE-NNSA. This work was, in part, supported by the US DOE under contract # DE-AC52-06NA25396. We also like to thank HPCAT and CHESS beamline staff for their assistance, especially Drs. H.-P. Liermann and S. V. Sinogeikin for their assistance in setting up heating experiments.

## References

- [1] D. Bancroft, E. L. Peterson, and S. Minshall, *J. Apply. Phys.* **27**, 291 (1956).
- [2] H. K. Mao, W. A. Bassett, and T. Takahashi, *J. Appl. Phys.* **38**, 272 (1967).
- [3] J. C. Jameson, Crystal Structures of Titanium, Zirconium, and Hafnium at High Pressures, *Science* **140**, 72 (1963).
- [4] F. E. Wang, W. J. Buehler, and S. J. Pickart, *J. Appl. Phys.* **36**, 3232 (1965).
- [5] S. K. Sikka, Y. K. Vohra, and R. Chidambaram, *Prog. Mater. Sci.* **27**, 245 (1982).
- [6] Y. K. Vohra, *Acta Metall.* **27**, 1671 (1979).
- [7] R. G. Hennig, D. R. Trinkle, J. Bouchet, S. G. Srinivasan, R. C. Albers and J. W. Wilkins, *Nature* **4**, 129 (2005).
- [8] Y. K. Vohra, S. K. Sikka, S. N. Vaidya and R. Chidambaram, *J. Phys. Chem. Solids* **38**, 1293 (1977).
- [9] T. Hattori, H. Saitoh, H. Kaneko, Y. Okajima, K. Aoki and W. Utsumi, *Phys. Rev. Lett.* **96**, 255504 (2006).
- [10] S. Merkel, N. Miyajima, D. Antonangeli, and G. Fiquet, *J. Appl. Phys.* **100**, 023510 (2006).

- [11] W. J. Nellis, J. A. Moriarty, A. C. Mitchell, M. Ross, R. G. Dandrea, N. W. Ashcroft, N. C. Holmes, and G. R. Gathers, Phys. Rev. Lett. **60**, 1414 (1998).
- [12] R. G. McQueen, S. P. Marsh, J. W. Taylor, J. M. Fritz, and W. J. Carter, in High Velocity Impact Phenomenon, edited by Kinslow R (Academic, New York, 1970), Chap. VII.
- [13] D. Errandonea, Y. Meng, M. Somayazulu, and D. Häussermann, Physica B **355**, 116 (2005).
- [14] E. Cerreta, G. T. Gray III, R. S. Hixson, P. A. Rigg, and D. Brown, Acta Materialia **53**, 1751 (2005).
- [15] D. R. Trinkle, R. G. Hennig, S. G. Shrinivasan, D. M. Hatch, M. D. Jones, H. T. Stokes, R. C. Albers, and J. W. Wilkins, Phys. Rev. Lett. **91**, 025701 (2003).
- [16] H. R. Wenk, S. Matthies, R. J. Hemley, H. K. Mao, and J. Shu, Nature **405**, 1044 (2000).

## Tables and Figures

TABLE I. Sample purity of zirconium samples studied (Wt ppm). All three samples have initial grain size of 25  $\mu\text{m}$ . Also included is the measured pressure at the start of the  $\alpha \rightarrow \omega$  transition under both non-hydrostatic and hydrostatic conditions.

|       | Hf     | Fe    | Al  | V   | O     | N   | C   | $P_{\alpha \rightarrow \omega}$ (GPa)<br>non-hydro. | $P_{\alpha \rightarrow \omega}$ (GPa)<br>hydro. |
|-------|--------|-------|-----|-----|-------|-----|-----|---|---|
| ZrI   | 35     | <50   | <20 | <50 | <50   | <20 | 22  | 4.6   | 6.4   |
| ZrII  | 350    | 125   | <20 | <25 | 390   | 15  | 70  | 5.5   | 7.5   |
| ZrIII | 14,000 | 2,400 | -   | -   | 1,200 | 80  | 270 | 10.8  | 11.6  |

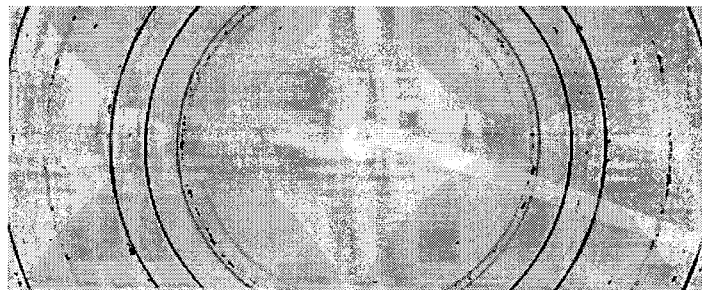


FIG. 1. Angle dispersive x-ray diffraction image collected from mid purity zirconium, ZrII. Image was collected during the start of the  $\alpha \rightarrow \omega$  transition at 7.5 GPa under hydrostatic conditions. Bragg spots are from  $\omega$  phase, while the full rings are from  $\alpha$  phase of zirconium and copper pressure marker.

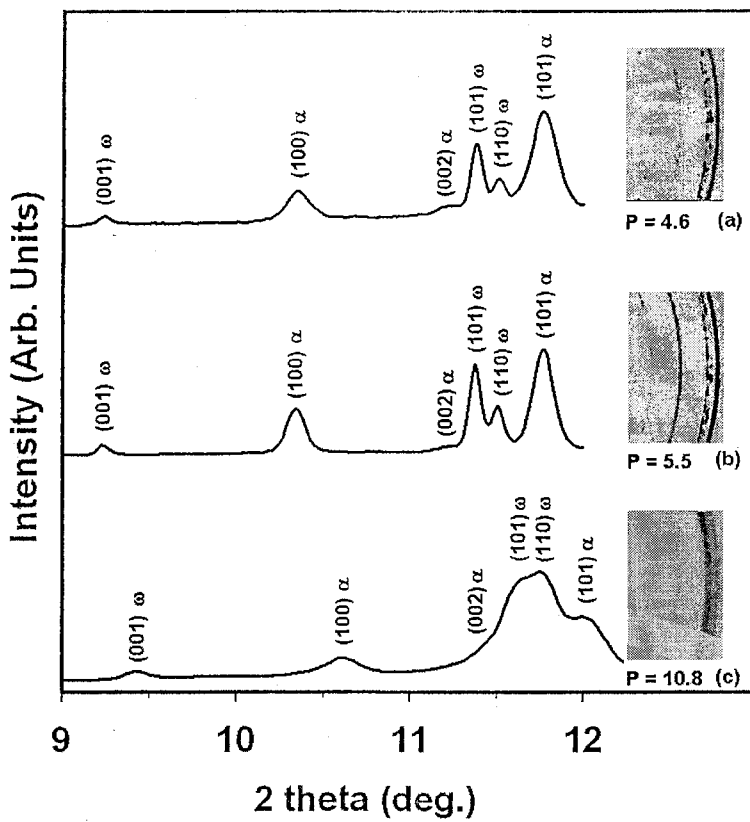
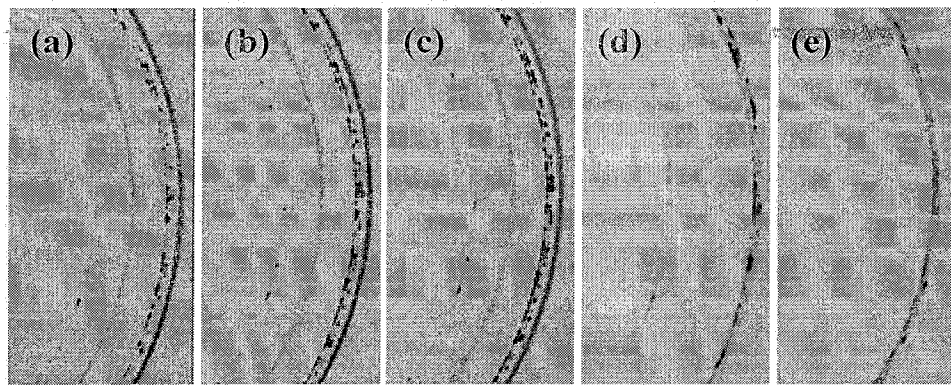
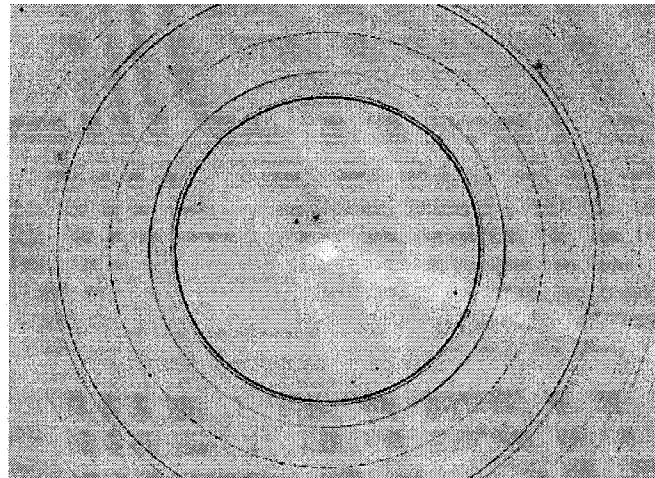


FIG. 2. Spectra collected at the start of the  $\alpha \rightarrow \omega$  transition for three different zirconium samples. Corresponding image plate reading is also included next to each spectrum. Large grain growth is observed for the two highest purity samples ZrI (a) and ZrII (b), but not the lowest purity sample, ZrIII (c).



**FIG. 3. Grain growth effects observed during room temperature compression of highest purity sample (ZrI), studied under non-hydrostatic conditions. (a), (b), and (c) were all taken at constant pressure during  $\alpha \rightarrow \omega$  transition at 4.6 GPa (see text for additional information). As the pressure is increased to 13.4 GPa only diffraction spots from  $\omega$  phase are observed (d). Decompression to ambient pressure indicates that the sample is a mixture of  $\alpha$  and  $\omega$  phases and  $\omega$  phase still appears grainy (e).**



**FIG. 4. ZrIII heated to 1279 K at 10.8 GPa undergoes  $\omega \rightarrow \beta$  transition; however, no significant grain growth is observed.**